applied sciences

MDPI

Article

Use of Urea-Modified Activated Carbon Sorbents Derived from Plant Residues for Gas Sorption

Almagul Kerimkulova [1,2], Yersultan Yermoldanov [2,3], Aitugan Sabitov [2,4,*], Leticia F. Velasco [5], Nazym Asanbek [2,3], Aisamal Kubaiden [2,3], Assem Zhumagaliyeva [2], Zulkhair Mansurov [3], Meiram Atamanov [2,3], Gulnur Nysanbayeva [3,6], Vadim Yermolenko [3] and Ospan Doszhanov [2,7]

1 Department of Materials Science, Nanotechnology and Engineering Physics, Satbayev University, Satbayev Str., 22a, Almaty 050013, Kazakhstan; almusha_84@mail.ru
2 Institute of Combustion Problems, Bogenbay Batyr 172, Almaty 050012, Kazakhstan; eursultanermoldanov@gmail.com (Y.Y.); naziko-asanbek@mail.ru (N.A.); kubaiden_aisamal2@live.kaznu.kz (A.K.); assemzhumagali@gmail.com (A.Z.); amk1310@mail.ru (M.A.); ospan.doszhanov@mail.ru (O.D.)
3 Faculty of Chemistry and Chemical Technology, Farabi University, Al-Farabi Ave. 71, Almaty 050040, Kazakhstan; zmansurov@kaznu.edu.kz (Z.M.); gulnur.83.29@mail.ru (G.N.); vadim_27_05@mail.ru (V.Y.)
4 Faculty of Natural Sciences, Kazakh National Women's Teacher Training University, Gogol Str., 114, k. 1, Almaty 050000, Kazakhstan
5 Department of Chemistry, Royal Military Academy, Avenue de la Renaissance 30, 1000 Brussels, Belgium; leticia.fernandezvelasco@mil.be
6 Department of General Education Disciplines, Civil Aviation Academy, Akhmetov Str. 44, Almaty 050039, Kazakhstan
7 Department of Automation and Robotics, Almaty Technological University, Tole bi Str. 100, Almaty 050012, Kazakhstan
* Correspondence: aitugans@mail.ru

Abstract

The growing demand for efficient and sustainable materials for air purification has stimulated interest in activated carbons derived from renewable biomass resources. In this study, activated carbons were prepared from Rice Husk, Wheat Straw, Sawdust, and Walnut shells and systematically investigated as sorbents for toxic gases and volatile organic compounds. The materials were characterized using nitrogen and water vapor sorption isotherms, scanning electron microscopy, thermogravimetric analysis, Fourier-transform infrared spectroscopy, energy-dispersive X-ray and XPS analysis to evaluate their textural properties, morphology, thermal stability, and surface chemistry. The results showed that the precursor type strongly influences the pore structure and functional group composition of the activated carbons. Wheat straw and Rice Husk-derived activated carbons exhibited the highest total pore volume and a well-developed porous structure, together with a high content of oxygen- and silicon-containing elements. Gas breakthrough experiments with different probes showed that Wheat Straw-derived activated carbon excels in non-polar VOC—cyclohexane removal due to its highly microporous structure. In contrast, Rice Husk-derived activated carbon displays strong affinity toward inorganic gases such as NH_3 and, after urea modification, achieves enhanced performance for SO_2. These results underscore the versatility and practical applicability of carbon materials obtained from plant residues.

Keywords: activated carbon; plant residues; urea; sorption; toxic gases

Check for updates

Academic Editor: Francis Verpoort

Received: 21 May 2026
Revised: 29 June 2026
Accepted: 5 July 2026
Published: 7 July 2026

Copyright: © 2026 by the authors. Licensee MDPI, Basel, Switzerland. This article is an open access article distributed under the terms and conditions of the Creative Commons Attribution (CC BY) license.

1. Introduction

Toxic gases and volatile substances pose serious risks to both the environment and human health. The content of toxic substances increases due to production factors in industry, as well as a result of geological shifts and natural phenomena. Natural pollution processes include volcanic eruptions, wildfires, reactions initiated by lightning discharges [1,2]. Anthropogenic sources can be divided into the following groups: energy production (fuel combustion) [3,4], transport (land, water and air) [5,6], technological processes (oil refineries, chemical industry, metallurgy, coal industry) [7,8] and households (methane emissions from livestock breeding, VOCs (volatile organic compounds) formation by veterinary drug degradation) [9–11].

The main pollutants are nitrogen and sulfur compounds (NOx, SOx, H_2S), carbon dioxide, carbon monoxide, hydrocarbons (methane, propane, cyclohexane), and other volatile organic compounds (chlorinated hydrocarbons CHxCly, formaldehyde and HCN).

Adsorption is becoming increasingly valuable among other well-known methods for cleaning industrial emissions, as it allows for the removal of almost all pollutants from gas streams. Solid materials with an enlarged surface, made in the form of granules or fine-grained materials, are usually used as adsorbents. Carbon materials are one of the main sources of sorbents used to purify industrial emissions from toxic and volatile compounds. Any organic compounds with a high carbon content can be sources of activated carbons. The growing industrial demand for carbon-containing sorption materials, along with the depletion of fossil resources and stricter environmental requirements, prompted the search for new precursors for the production of activated carbons. Plant waste such as Rice Husks, Wheat Straw, Walnut shells, and others can be considered very promising, economically profitable, and permanently renewable sources [12–14]. Apart from porous sorbents, alternative high-value utilization pathways for various regional biomass resources have recently extended into the development of functional structural materials and barrier films [15,16].

While the retention of organic compounds on carbon sorbents is mainly governed by physiorption, the removal of inorganic species often benefits from the presence of reactive surface sites. These can be introduced through impregnation with suitable compounds—such as transition—especially for gases like NOx, SOx and H_2S, although for others, including NH_3, milder surface treatments that adjust the surface chemistry are sufficient.

In this work, activated carbons obtained from Rice Husk, Wheat Straw, Sawdust and Walnut shells were evaluated for the removal of non-polar VOCs and inorganic gases. Some of these materials were further modified to enhance their performance, and several of them showed promising results for potential use in gas-filter applications. The discussion of the results is grounded in their porosity, surface chemistry and composition, as revealed by the thorough characterization performed.

2. Materials and Methods

2.1. Raw Materials

Wheat straw, coniferous Sawdust, and Rice Husks collected in the Almaty region, and Walnut shells collected in the Medeu district Almaty city were used as the main raw materials for the development of porous sorbents.

2.2. Carbonization of Raw Materials

The carbonization process of the raw materials was conducted in a steel reactor, which was placed inside a vertical furnace equipped with a thermocouple. Before the starting heating process, nitrogen was allowed to flow for 30 min to remove the air in the tube, after

which the temperature was increased. The samples were heated to 850 °C for 120 min with controlling heating rate 3 °C/min, after which the temperature was lowered to 650 °C and maintained for an additional 90 min. Once the heating stage was complete, the samples were gradually cooled to room temperature. This method facilitated the formation of a porous structure in the carbon material and helped in the removal of volatile compounds.

After carbonization, the samples were boiled in distilled water to eliminate any residual impurities. This boiling process was performed at a temperature of 95–100 °C on a laboratory stove with constant stirring, which enhanced the effective removal of undesirable water-soluble compounds. Following this, the samples were dried in a drying cabinet at a temperature of 100–105 °C until all moisture was completely removed. This stage ensured the stabilization of the material's structure prior to further use.

2.3. Activation of Carbonized Raw Material Samples

Carbonized samples were activated with the addition of NaOH in a 1:2 mass ratio (alkali/sorbent). Pre-mixed samples of carbonized material and alkali were left overnight in a drying cabinet at a temperature of 70 °C. Activation is carried out at a temperature of 850 °C for 120 min and then the temperature is gradually reduced to room temperature. The activation process takes place in a vertical steel furnace under an inert gas-argon blanket, which was constantly fed at a flow rate of 50 cm^3/min. The activated carbon obtained from plant wastes was washed with deionized water three times to remove the soluble ash content, including sodium salts doped in the activated carbon, which can block pores [17].

2.4. Modification of Activated Carbon Samples

The activated carbon is then mixed with a 30% urea solution in a 3:1 and 2:1 (urea/carbon) mass ratio and loaded into a mini-reactor with mechanical stirring YZPR-250M (BOYN, Hangzhou, China). The process takes place at a temperature of 180 °C in an inert nitrogen environment and under a pressure of up to 10 MPa to modify carbon samples by urea.

After the modification was completed and pressure was reduced to normal, samples were heated at the vertical furnace to the 600 °C to release non-bounded urea and water from carbon pores. Modified activated carbon was then washed with 10% hydrochloric acid to remove the impurities generated during the modification process, and then washed by deionized water several times [18].

2.5. Characterization of Activated Carbon

The chemical composition of the samples of activated and modified carbons was studied using scanning electron microscopy (SEM) "QUANTA 3D 200i" (FEI, Morristown, NJ, USA), in combination with an EDAX spectrometer and a semiconductor detector (EDAX, Mahwah, NJ, USA) with an energy tolerance of 128 eV (polymer material, sensitive area d = 0.3 mm).

The infrared spectra of the samples were recorded using a Spectrum 65, Perkin & Elmer 1100 FTIR spectrometer (Perkin & Elmer, Shelton, CT, USA) in the range of 4000–400 cm^{-1} using KBr granules with a resolution of 1 cm^{-1}. A pellet for infrared studies was obtained by mixing this sample with KBr crystals and pressing into a pellet.

Thermogravimetric analysis was conducted using a Mettler Toledo TGA–DSC 3+ instrument (Mettler Toledo, Greifensee, Switzerland) with a heating rate of 10 °C/min up to 900 °C.

The water isotherms were measured at a temperature of 20 °C using a gravimetric water sorption analyzer (Aquadyne DVS, Quantachrome Instruments, Boynton Beach, FL,

USA). Each point of the gravimetric isotherm was obtained after reaching an equilibrium time corresponding to a 0.0008% change in mass per minute at a given relative humidity.

To perform a detailed investigation of the sub-nanometer ultramicroporosity, CO_2 adsorption isotherms were recorded at 273 K, and Ar adsorption isotherms were measured at 87 K using an automatic volumetric porosimetry system. The micropore volume of the Walnut shell-derived sample was calculated from the CO_2 data via the Dubinin–Radushkevich method. The pore size distribution functions were evaluated by applying the Non-Local Density Functional Theory (NLDFT) slit-pore model to the CO_2 data and the Quenched Solid Density Functional Theory (QSDFT) slit-pore model to the Ar and N_2 data.

2.6. Gas Sorption Experiments

The experimental gas (NH_3 or SO_2) sorption unit was performed in accordance with the ISO 10121-1:2014 standard "Test Method for Assessing the Performance of Gas-Phase Air Cleaning Media and Devices for General Ventilation—Part 1: Gas-Phase Air Cleaning Media " [19]. The installation scheme is shown in Figure 1 as it was described in [20].

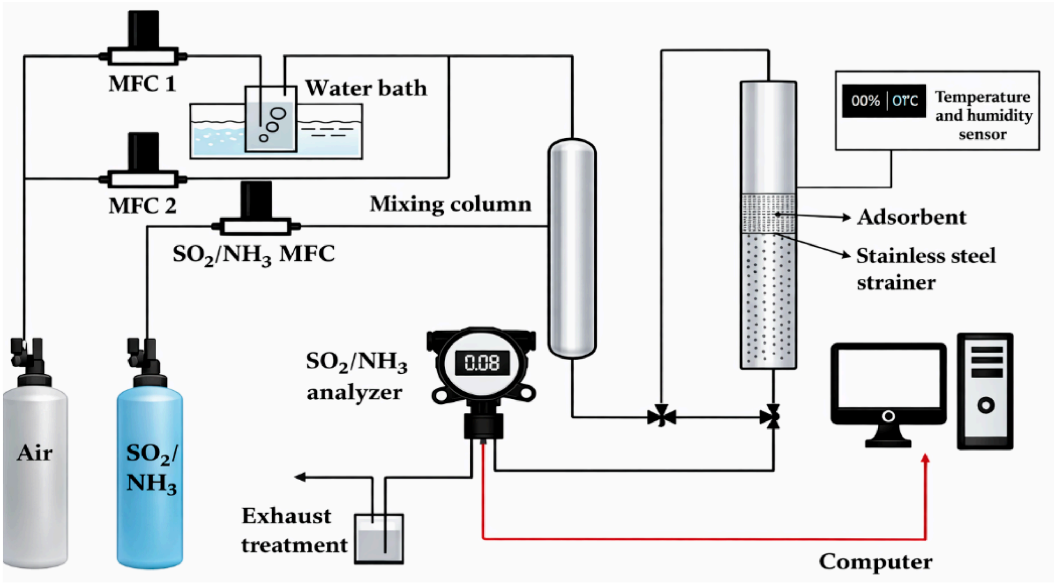


Figure 1. Scheme of the gas sorption experiments.

The conditions for conducting experiments on gas sorption are a temperature of 23 °C and a relative humidity of no more than 50%. The 4.5.0 L/min airflow was divided into two, while the 4 L/min airflow passed through a water bath and then mixed with the 0.495 L/min airflow containing the toxic gas (NH_3 or SO_2). The total humidity of the air and analyzed gas mixture was 50%, and the concentration of polluting gas was 90 ppm.

The resulting gas mixture was directed at a rate of 130 mL/s to an adsorption chamber, into which 3 g of carbon sorbent was placed; the current concentration is determined using an analyzer that outputs the results directly to a PC. The dynamic adsorption experiments were carried out until complete saturation of the sorbent bed was achieved, which was indicated by the outlet gas concentration matching the initial inlet concentration (=90 ppm). This allowed for the recording of full breakthrough curves and the subsequent calculation of both the breakthrough time and the total gravimetric sorption capacity. All samples were analyzed in at least three repetitions. The GT-FGA1000L (Allred, Qingdao, China) analyzer was used for controlling gas concentrations.

2.7. Thermal Regeneration of Modified Sorbents

The saturated adsorbent was regenerated within the microreactor by heating at 400 °C in an inert atmosphere. The regeneration duration was fixed at 60 min per cycle, ensuring

complete desorption of the adsorbate as confirmed by the stabilization of the effluent gas concentration to background levels. The pure sorbent sample was approximately 100 mg. A high-purity argon flow of 30 mL/min was maintained using a calibrated Sevenstar D07-series MFC (Beijing Sevenstar Flow Co., Ltd., Beijing, China), ensuring a stable flow rate and efficient removal of desorbed SO_2, while preventing the oxidation of the carbon framework. The effluent gas concentration was monitored in real-time using a GT-FGA1000L gas analyzer (Allred, Jiangmen, China). The system was configured with a bypass arrangement to prevent pressure fluctuations within the microreactor, and the analyzer recorded data at a frequency of 1 Hz, allowing for the precise integration of desorption peaks to quantify the mass of desorbed SO_2. The cyclic performance was assessed over 5 consecutive adsorption-regeneration cycles. To eliminate weighing errors and achieve high accuracy (±0.01 mg), the adsorbent was weighed directly in the quartz boat using an analytical microbalance. Between cycles, samples were cooled to room temperature in a desiccator to prevent moisture uptake.

3. Results and Discussion

3.1. Characterization of Activated Carbons Prepared from Plants Residues

The objective of this study was to analyze the porosity of the carbons obtained from plant wastes and determine their adsorption capacity for organic contaminants. Before the analysis, the materials were outgassed for 17 h at 120 °C and then nitrogen adsorption–desorption isotherms at −196 °C were recorded. Results of nitrogen sorption analysis are presented in Figure 2.

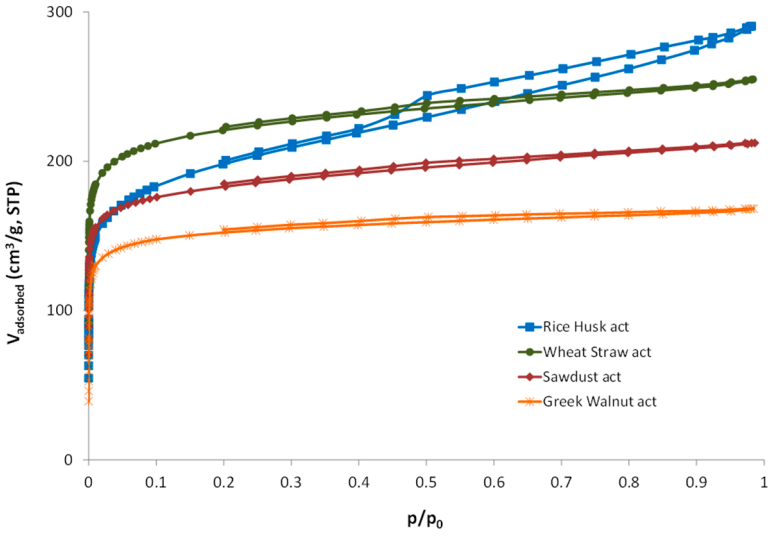


Figure 2. N_2 adsorption–desorption isotherms at −196 °C for the activated samples.

The isotherms of the activated Wheat Straw, Sawdust, and Greek Walnut carbon samples have a similar profile and do not intersect, showing a decrease in the adsorption capacity, respectively. These isotherms are typical of microporous materials. However, the shape of the isotherm of the activated carbon from the Rice Husk sample indicates a micro-mesoporous nature, achieving the highest total pore volume. On the other hand, the non-activated carbonized samples display a non-developed porosity. Moreover, the analysis was extremely slow, indicating a constricted access of the nitrogen.

In order to confirm the assumptions regarding the porous structure of the samples, the QSDFT model with slit pore geometry for carbon materials was applied, allowing the determination of the pore size distribution. The results of the analysis are shown in Figure 3.

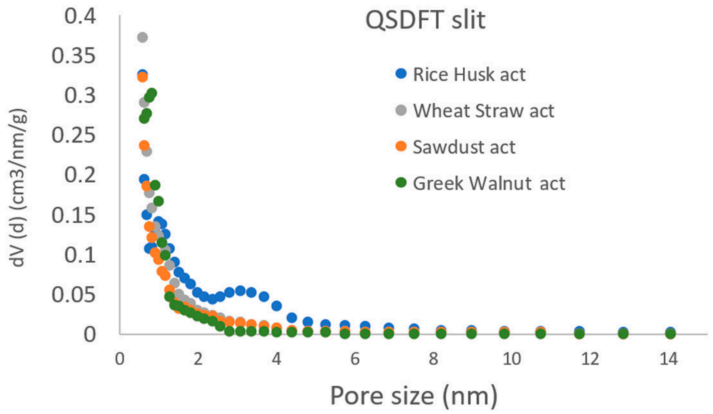


Figure 3. Pore size distribution of the activated samples obtained using the QSDFT slit pore equilibrium model for carbons.

In Figure 3, it is clearly observed that the sample with the highest presence of mesopores (pore width between 2 and 50 nm) is the Rice Husk activated sample. In this regard, it is worth noting that these are narrow mesopores, with a size smaller than 6 nm. It is also important to note that the other three samples exhibit very similar pore size distributions, although with different peak intensities. Similar characteristics of the distribution of meso- and micropores in carbonized plant samples with other methods of carbon activation are noted in the works of other authors [21–23].

Table 1 presents the textural parameters of the activated carbons prepared from various plant sources. The N_2 adsorption isotherms were used to determine the BET specific surface area (S_{BET}), the micropore volume (calculated using the Dubinin–Radushkevich equation), and the mesopore volume (obtained as the difference between the total pore volume and the micropore volume). The QSDFT results are presented to illustrate the micropore size distribution, distinguishing between ultramicropores (μmicro, with pore widths lower than 0.7 nm) and total microporosity.

Table 1. Textural parameters of the activated carbons calculated from the nitrogen isotherms.

Sample	S_{BET} (m^2/g)	C_{BET}	Total Pore Volume (cm^3/g)	Micropore Volume (cm^3/g)	Mesopore Volume (cm^3/g)	QSDFT Slit	
						$V\mu_{micro}$ DFT, cm^3/g	V_{micro} DFT, cm^3/g
Wheat Straw Act	859	1122	0.394	0.317	0.077	0.220	0.325
Sawdust Act	711	1777	0.328	0.266	0.062	0.193	0.270
Rice Husk Act	738	497	0.449	0.266	0.183	0.150	0.271
Greek Walnut Act	597	1724	0.260	0.234	0.026	0.116	0.226

Wheat Straw is the precursor that generates the highest microporosity (0.317 cm^3/g), together with the largest S_{BET} (859 m^2/g), whereas the Walnut-derived sample exhibits the lowest overall pore development, both in the micro- and mesopore ranges. Sawdust shows an intermediate behavior between these two extremes. In contrast, Rice Husks developed the largest total pore volume and the highest mesopore contribution (0.183 cm^3/g). Interestingly, despite the nearly identical micropore volumes of the Sawdust- and Rice Husk-derived carbons, the logarithmic isotherm plot and the QSDFT analysis reveal a higher proportion of ultramicropores in the former: 0.193 vs. 0.150 cm^3/g, respectively. This means that the Sawdust precursor enables a narrower microporosity than Rice Husk (Figure 3 and Table 1). The close agreement between micropore volumes calculated by DR and QSDFT confirms the consistency of the analysis.

Based on these results, activated Straw would be the optimal material for the adsorption of organic contaminants such as cyclohexane because highly microporous carbons are favored in non-polar VOC adsorption due to strong confinement and enhanced adsorption potentials. On the other hand, Rice Husk can be a good candidate for the retention of inorganic gases because micro-mesoporous carbons typically provide improved diffusion and accessibility. This will be further evaluated and discussed below.

The capacity values towards cyclohexane retention obtained after integrating the breakthrough time curves measured with an automatic DVS instrument (MixSorb S, 3P Instruments) operated under dry conditions are recorded in Table 2. As expected, the values follow the same trend as the one obtained for the BET specific surface area, being that activated Straw is the material with the highest capacity. This is due to the fact that cyclohexane is preferentially adsorbed in the micropores. It is worth noting that the capacity calculated for the walnut-based material is lower than what could be potentially expected. This behavior may be attributed to a less interconnected pore structure, which hinders cyclohexane accessibility, and/or to a significant fraction of very narrow ultramicropores that are not accessible to the target compound.

Table 2. Sorption capacities of the activated carbons towards cyclohexane.

Sample	Capacity (mmol Ciclohex/g Carbon)
Wheat Straw Act	1.829
Sawdust Act	1.381
Rice Husk Act	1.500
Greek Walnut Act	0.727

To definitively validate this hypothesis, additional CO_2 (273 K) and Ar (87 K) adsorption analyses were performed for the Walnut shell-derived activated carbon (Figure 4).

The micropore volume calculated from the CO_2 isotherm reached 0.233 cm^3/g, confirming a profound contribution of extremely narrow micropores. This structural feature is clearly highlighted by the combined $CO_2 \backslash N_2$ pore size distribution curve (Figure 4b), which reveals a high volume of pores with diameters strictly below 0.6 nm. Because these ultramicropores are geometrically smaller than the kinetic diameter of cyclohexane (~5.6 A), they remain completely steric-hindered and inaccessible to the volatile organic molecule, perfectly explaining the lower dynamic VOC breakthrough capacity. Furthermore, the PSD obtained from the Ar isotherm at 87 K (Figure 4c) matches the nitrogen-based profile, demonstrating a highly developed sub-nanometer framework, with slight shifts legally attributed to the absence of a quadrupole moment in spherical Ar atoms, which allows a more accurate geometric assessment free from specific interactions with surface functional groups.

Similarly, the sorption performance of the activated Rice Husk towards cyclohexane appears to be enhanced compared to Sawdust, likely due to the presence of a mesoporous network that improves the accessibility of the organic molecule to preferential adsorption sites, as well as a lower fraction of such inaccessible ultramicropores.

Figure 5 presents scanning electron microscopy (SEM) images of activated carbon samples produced from various plant materials. Figure 5a shows the sample form of straw, which has a more fibrous and less macroporous structure than Rice Husk carbon. This fibrous nature is likely due to the retention of the original plant cell structure during the carbonization process, contributing to the mechanical strength of the activated carbon.

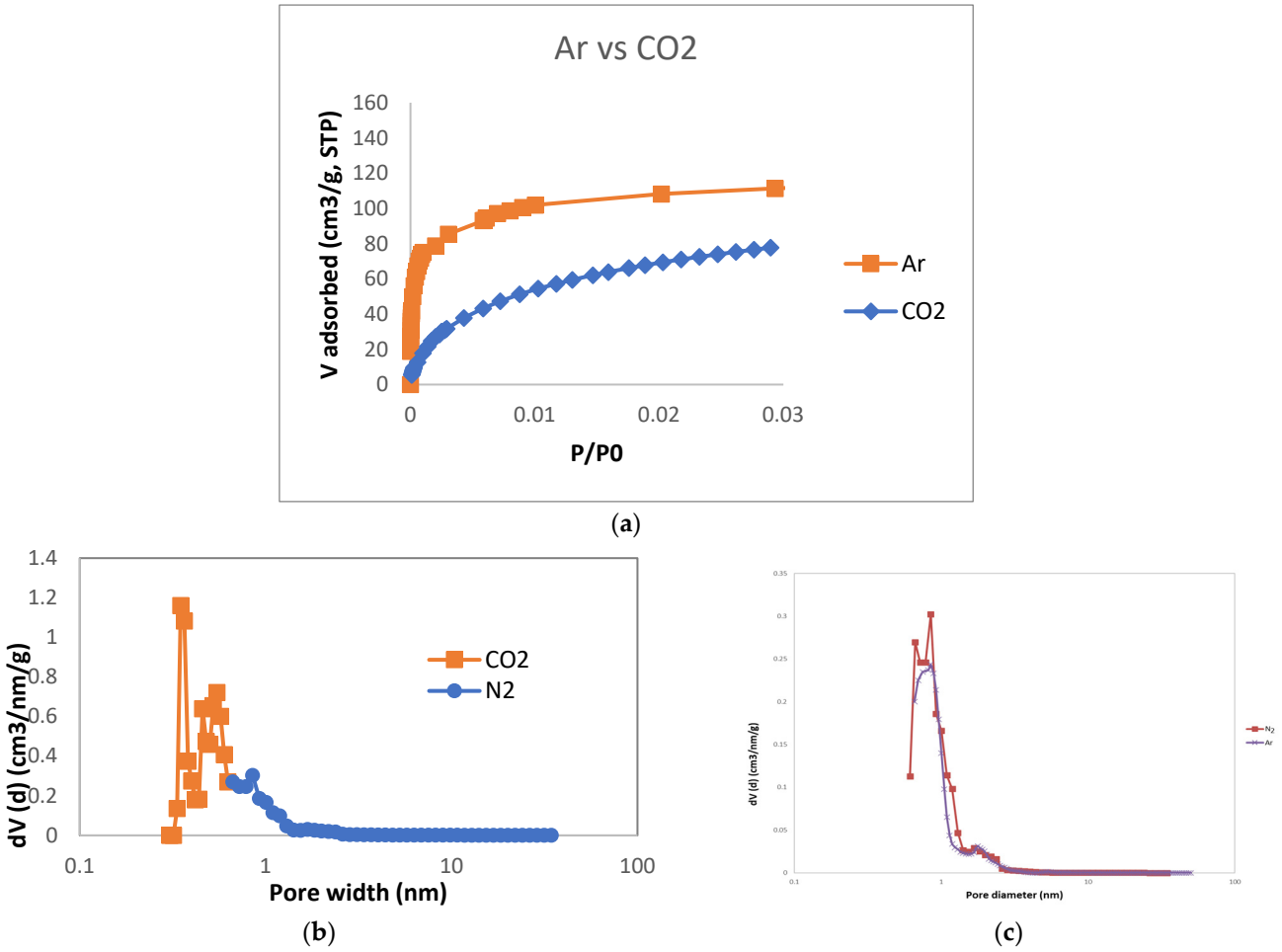


Figure 4. Advanced porosimetry characterization of the Walnut shell-based activated carbon: (**a**) CO_2 (273 K) and Ar (87 K) adsorption isotherms; (**b**) combined CO_2\N_2 PSD evaluated via NLDFT/QSDFT slit-pore models; (**c**) comparison of the PSD functions obtained from Ar and N_2 adsorption data using the QSDFT model.

The structure of this material makes it suitable for use as a mechanically stable material, especially in applications where preserving structural integrity is essential for effective gas filtration while avoiding damage to the filter medium.

Figure 5b illustrates activated carbon derived from Sawdust. The activated carbon exhibits a more elongated and layered structure, with visible grooves and channels on its surface. This suggests that the original fibrous structure of the Sawdust has been partially preserved during the heating process. This layered structure could potentially serve as pathways for water and nutrient transportation, making the activated carbon beneficial for agricultural purposes.

In contrast, Figure 5c presents activated carbon produced from Rice Husks. This activated carbon displays a highly porous structure, characterized by numerous macropores as observed in the SEM images, as well as smaller cavities and interconnected networks inferred from nitrogen adsorption isotherms. This porosity is a result of the thermal decomposition of organic matter during the carbonization process. Due to its high overall porosity and the presence of an interconnected porous structure, Rice Husk-derived activated carbon is lightweight and suitable for applications requiring high levels of adsorption, such as the removal of pollutants from air.

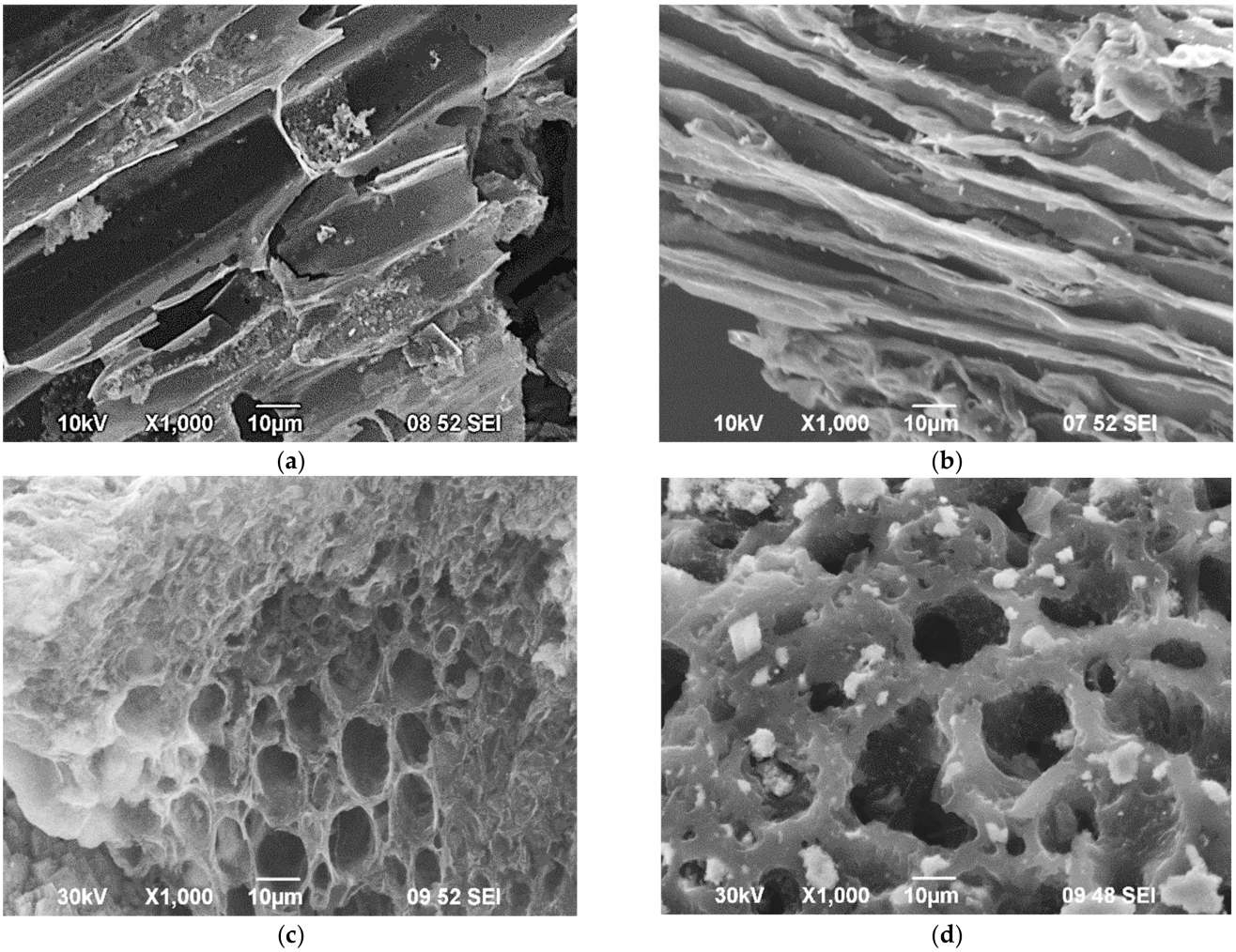
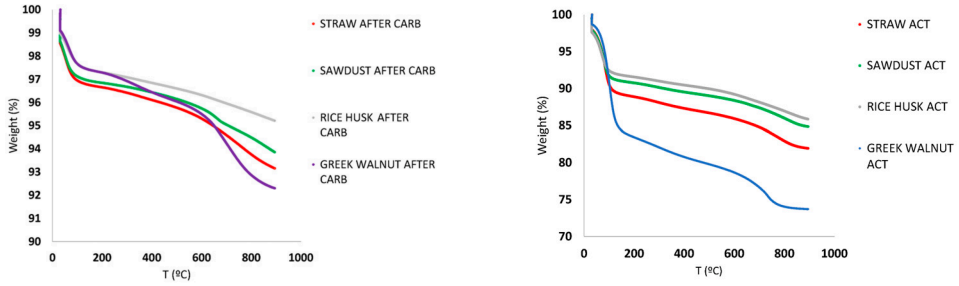


Figure 5. SEM images of activated carbon samples: (**a**) Wheat Straw; (**b**) Sawdust; (**c**) Rice Husk; (**d**) Greek Walnut.

Figure 5d illustrates a Walnut shell-derived activated carbon, which also exhibits a fibrous structure, although with larger visible pores and cavities compared to Rice Husk-based biochar. These features suggest that walnut biochar may be well-suited for the adsorption of high molecular weight organic substances due to its porosity. Despite this, the structure remains intact, indicating that this biochar could still offer benefits in terms of soil aeration and water retention [24].

In industry, the process of filtering gases and volatile substances with sorbents often occurs at high temperatures, and therefore, the materials used for sorption must be temperature-stable. The following graphs show the thermogravimetric results, illustrating the evolution of the sample weights with temperature in an inert atmosphere (Ar). The samples were heated up to 900 °C, with a heating ramp of 10 °C/min (Figure 6).

The first observation is that, as expected, activated samples lose more mass than carbonized samples as temperature increases, which can be attributed to a higher number of surface groups in activated samples. Among these, the activated walnut sample shows the greatest mass loss. When comparing Figure 6a,b, it is evident that curves generally follow a similar trend, except for the walnut activated sample, which shows a noticeably steeper slope and drops below other curves at an earlier stage.



(**a**) (**b**)

Figure 6. TG profiles of the carbonized (**a**); activated (**b**) carbon samples.

In order to study the nature of the lateral functional groups, we performed an IR analysis of all activated carbon samples (Figure 7). As expected, all four samples have characteristic peaks of hydroxyl groups (-OH) in the region of 3300–3500 cm^{-1}, as well as carboxyl and carbonyl groups (-C=O) in the region of 1650 cm^{-1}. Carboxyl and carbonyl groups in activated carbon samples appear during the thermal treatment of plant samples—in the process of high-temperature pyrolysis. The above-mentioned functional groups may be responsible for the chemical interaction of activated carbon with positively charged groups of the sorbed samples, for example with ammonia, ammonium containing compounds, as well as with metal cations.

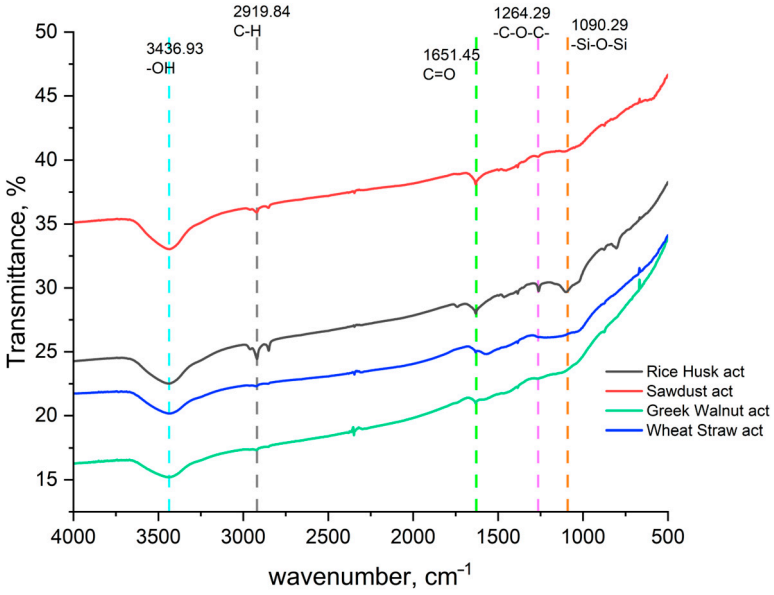


Figure 7. FTIR—spectra of the activated carbon samples.

However, there are also minor differences in the IR spectra of the analyzed samples. Thus, the carboxyl/carbonyl peak in the Wheat Straw sample is wide and shifted to the long-wavelength side, and the peak is located at a wavenumber of 1500–1600 cm^{-1}. Additionally, the band at 2860–2920 cm^{-1} corresponds to C-H stretching, further indicating the presence of aliphatic hydrocarbons in Sawdust and Rice Husk.

Activated carbon from Rice Husks and Wheat Straws also has a slight peak in the range of 1250–1300 cm^{-1}, which is typical for functional groups of -C-O-C-—valence vibrations in esters.

An important and significant difference in activated carbon sample from the Rice Husks is a wide peak at a wave number of 1000–1100 cm^{-1}, which is a parameter indicating the manifestation of silica (Si–O–Si) structures. A similar, but not distinct broad peak is

observed in the spectrum of Wheat Straw and Walnut shell samples at 1200–1050 cm^{-1}, which may also indicate the presence of silicon-related groups [25,26].

These changes confirm that activation promotes the introduction of oxygen-containing functional groups and improves the structural organization of the material, including the porosity of the surface.

In order to study the effect of oxygen groups on the surface properties of activated carbon samples, we studied their ability to adsorb water vapor at different ambient humidity levels (Figure 8).

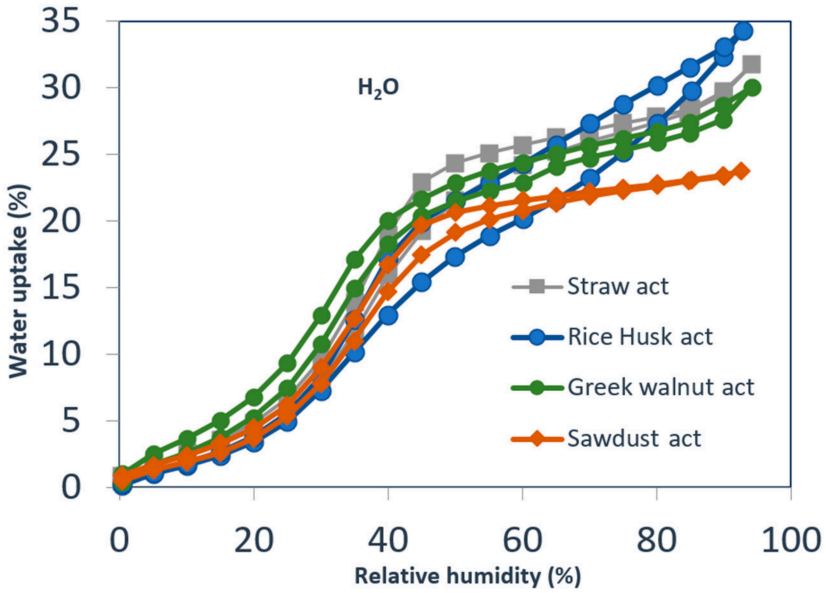


Figure 8. Water vapor sorption isotherms at 20 °C of the activated carbon samples: (blue line) Rice Husk act; (gray line) Straw act; (red line) Sawdust and (green line) Walnut shells.

Figure 8 clearly shows that Greek Walnut is the most hydrophilic material, as it exhibits the highest sorption capacity at low relative humidity, where surface chemistry governs water vapor adsorption. This behavior is consistent with the TG profiles (Figure 6b), which show the most intense drop around 150 °C for the activated Walnut, indicating a higher amount of strongly adsorbed water compared to the other samples.

Moreover, it displays a total water uptake comparable to that of activated Straw, despite the latter having a more developed porosity (Table 1). At higher relative humidity, porosity becomes the dominant factor controlling water uptake, as observed for the Rice Husk and straw samples, which reach values of about 32–34% at relative humidity above 90%. In contrast, the Sawdust sample shows the lowest water vapor adsorption at high relative humidity.

It should be emphasized that the total water uptake in a water vapor sorption isotherm is governed by distinct phenomena depending on the relative pressure range. In carbon-based matrices, surface chemistry dominates the initial region of the isotherm (RH < 40%), where oxygen and nitrogen functional groups act as primary hydrophilic adsorption sites. Within this low-to-moderate moisture window, Rice Husk act exhibits the lowest vapor uptake, reflecting a more hydrophobic surface framework and a lower density of primary nucleation centers compared to alternative materials.

Conversely, at intermediate and high relative humidity (RH > 80%), the pore-filling mechanism and capillary condensation become the controlling factors. Since Rice Husk act possesses the highest total porosity and pore volume among the investigated samples, it physically accommodates a larger volume of condensed water at near-saturation pressures, resulting in a higher ultimate uptake than that of Sawdust [27].

In order to confirm the presence of silicon, oxygen and other compounds in activated carbon samples, EDAX analysis was performed (Figure 9).

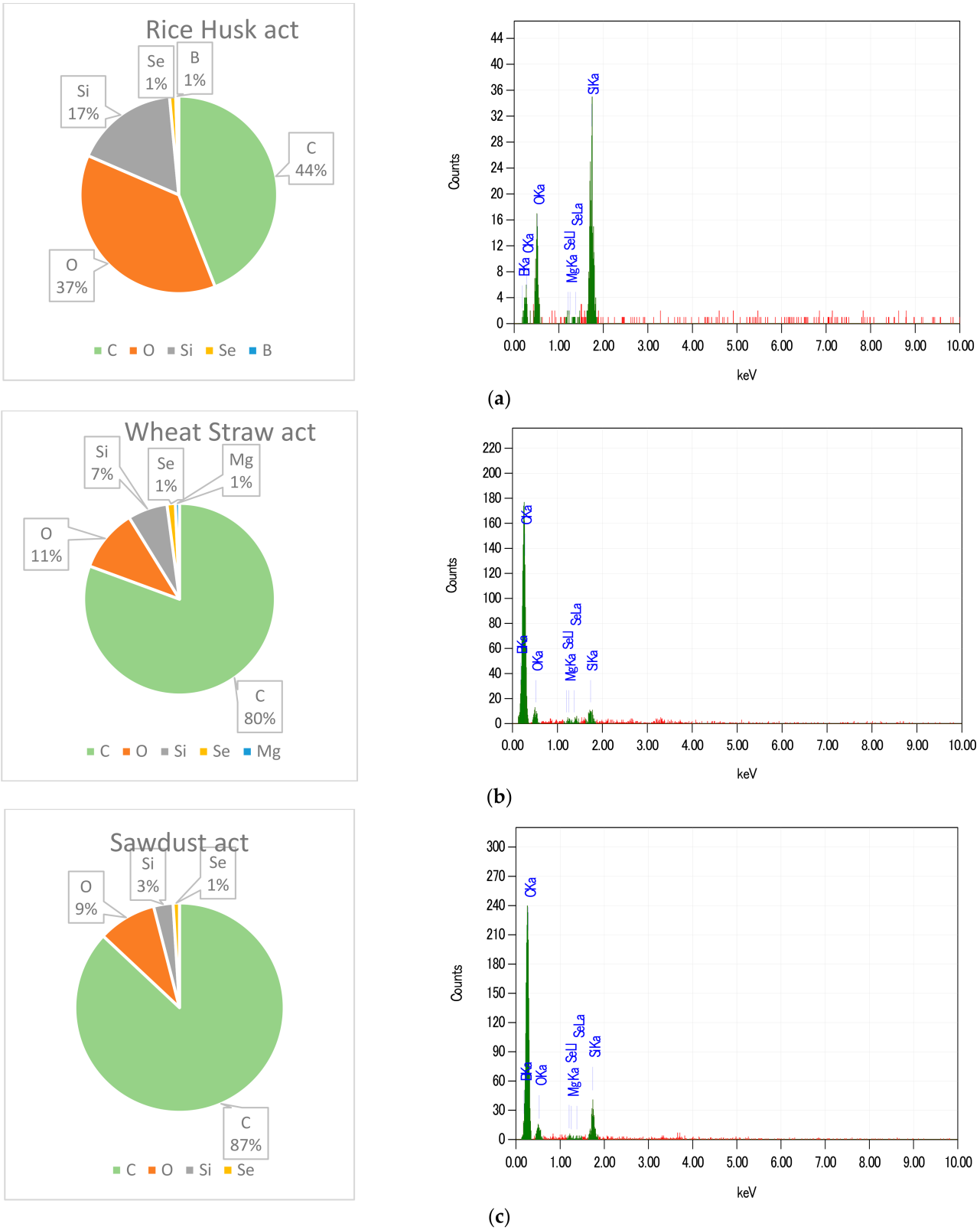


Figure 9. *Cont.*

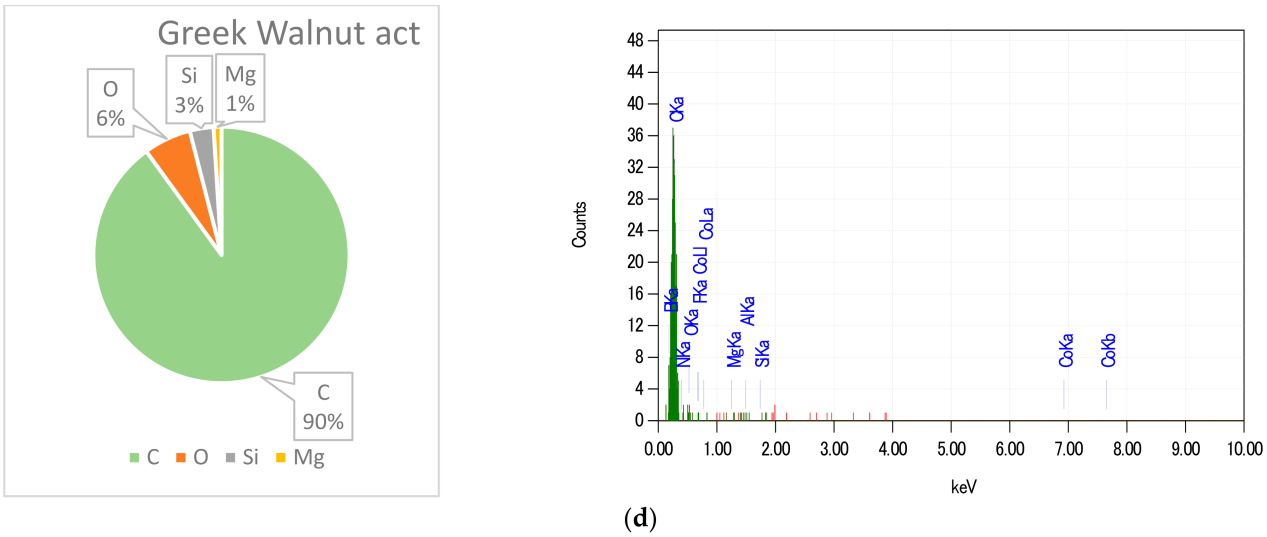


Figure 9. EDAX analysis results of the activated carbon samples: (**a**) Rice Husk act; (**b**) Straw act; (**c**) Sawdust and (**d**) Walnut shells.

The results of the EDAX analysis confirmed the results of the FTIR spectra regarding the presence of silicon compounds in activated carbon samples in Rice Husk (Figure 9a) and Wheat Straw (Figure 9b). Thus, the content of silicon atoms in Rice Husks is up to 17%, and in Wheat Straw 5%, respectively.

A very important fact is that the oxygen content in the Rice Husk sample is up to 37%, which may be directly related to the increased bonding of silicon atoms and compounds such as Si–O–Si (silica, silicates), Si–O–C at the carbon–silica interface, aromatic C–O–C (ethers), and conjugated C=O in a highly stabilized carbon matrix. These oxygen-containing groups did not act valuably on hydrophilic properties of the Rice Husk sample surface. Otherwise, a higher mass loss during the thermogravimetric analysis and a higher water uptake should be observed.

The content of silicon compounds is also confirmed in the Sawdust and Walnut shell samples and reaches up to 3% (Figure 9c,d). Also, in activated carbon samples from Wheat straw and Walnut, the presence of Mg atoms in the 1% ratio was found. Magnesium (Mg) is an essential macronutrient for plant growth, serving as the central atom in the chlorophyll molecule, which enables photosynthesis [28–30].

Summarizing the results of nitrogen and water adsorption, SEM, TG, FTIR and EDAX, activated Straw and Rice Husk samples are the most interesting. Straw, displaying the largest micropore volume, is certainly the best material for cyclohexane adsorption, since microporosity largely determines the overall adsorption capacity, and promotes strong physical interactions with the adsorbed molecules. This was further confirmed by breakthrough experiments with cyclohexane. On the other hand, Rice Husk, which has the largest total pore volume and the lowest hydrophilicity, is an interesting material, especially when conducting experiments in conditions of high humidity [31–33].

3.2. Sorption of NH_3 on Various Carbon Samples

The sorption of ammonia was studied to evaluate the applicability of the activated carbon samples for the removal of inorganic gases. Ammonia sorption results are shown in Figure 10, and the corresponding breakthrough times are listed in Table 3.

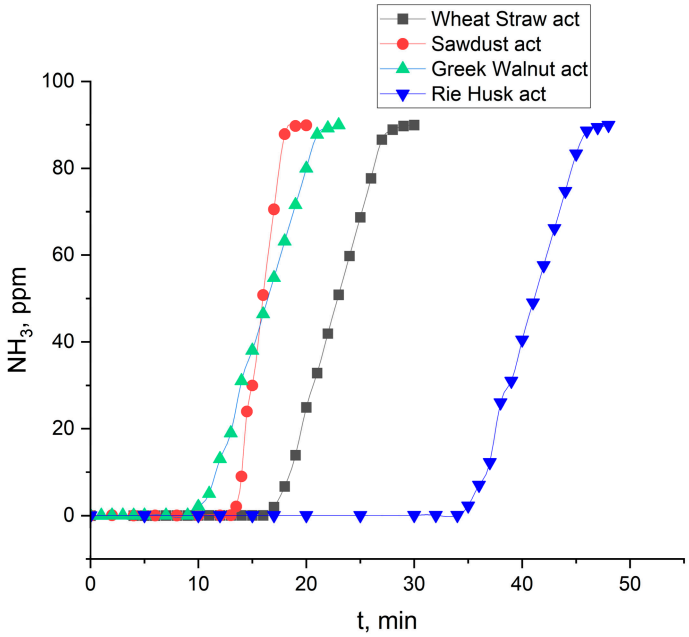


Figure 10. NH_3 breakthrough time curves of activated carbon samples.

Table 3. NH_3 breakthrough times and adsorption capacity of activated carbon samples.

Samples	Breakthrough Time, Min (NH_3—2 ppm)	Time (Conc. NH_3—25 ppm)	q_{total} (mg/g)
Greek Walnut act	10 min 25 s	13 min 54 s	2.03
Rice Husk act	35 min 45 s	39 min 40 s	6.02
Wheat Straw act	17 min 12 s	20 min 9 s	3.17
Sawdust act	13 min 40 s	14 min 25 s	2.36

As can be seen from Figure 10 and Table 3, the Rice Husk act sample has the maximum ammonia breakthrough time and ranges from 36 (2 ppm NH_3) to 40 min (25 ppm NH_3). Breakthrough time is a characteristic parameter of the sorbent that reflects its ability to retain the sorbed gas. The longer the breakthrough time, the higher the sorption capacity of the material, in this case for ammonia. Walnut shell and Sawdust samples exhibit the lowest breakthrough times at both 2 and 25 ppm, which can be attributed to their less developed porosity, limiting ammonia adsorption that is largely governed by physio sorption. However, surface chemistry also plays a role in ammonia sorption.

It is important that the recorded dynamic sorption capacities (reaching 6.02 mg/g for the Rice Husk act sample) were obtained under conditions of increased hydrodynamic stress. The volumetric flow rate of 7.8 L/min with a low sorbent weight (3.0 g) creates a high specific flow rate of the gas mixture—about 2.6 L/(min × g). In dynamic adsorption processes in a stationary layer, such an intensive regime dramatically reduces the contact time of the phases and inevitably stretches the mass transfer zone.

The fact that activated carbon from Rice Husks demonstrates such a long protective action time (up to 40 min) indicates a high kinetic availability of its porous structure. The developed micro-mesoporous architectonics of the material ensures effective internal diffusion of polar ammonia molecules.

In this regard, the Rice Husk act is an excellent sorbent for ammonia sorption due to the following reasons: (i) it has a well-developed and interconnected porous structure, with the highest total pore volume and (ii) according to TG analysis and water sorption isotherms, it is the most hydrophobic material, which is particularly advantageous under the humid conditions used in these experiments, as it minimizes competition between

water and ammonia for the available adsorption sites. Based on these results and according to the classification in [34], gas masks using Rice Husk activated carbon can be classified as K2-type sorbents for ammonia.

3.3. Urea Modified Rice Husk Activated Carbon Properties

As the activated Rice Husk sample shows higher breakthrough time values for ammonia, it appears particularly promising as a more universal sorbent for inorganic gases. In this context, its surface was further modified using urea to enhance its affinity toward acidic gases such as SO_2, while aiming at preserving a hierarchical pore structure composed of macropores, mesopores, and micropores, which facilitates the diffusion of target molecules toward the adsorption sites [17]. Nitrogen sorption isotherms of Rice Husk before and after modification with urea are presented in Figure 11.

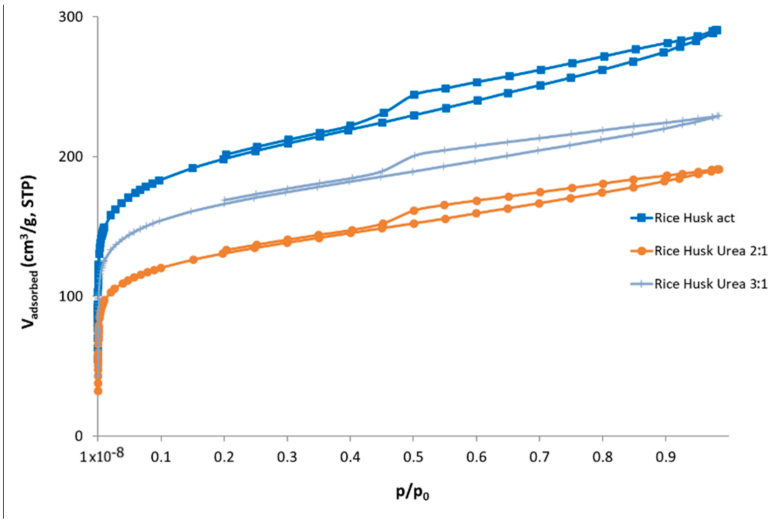


Figure 11. Nitrogen sorption isotherms of the Rice Husk-based activated carbons by urea at the 2:1 and 3:1 carbon/urea mass ratio.

It can be clearly seen that the impregnation with urea negatively affects the textural properties of the initial material. However, the isotherm profiles remain very similar, still indicating the presence of both micropores and mesopores, albeit to a lesser extent.

The pore size distributions (Figure 12) further support this observation, showing nearly identical qualitative profiles, though with slight quantitative differences.

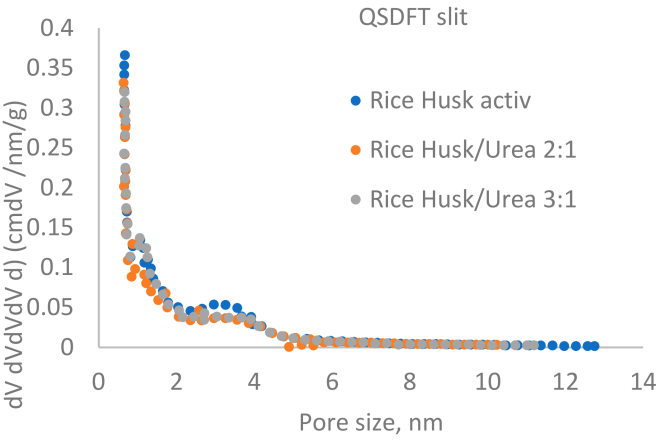


Figure 12. QSDFT slit equilibrium model analysis of Rice Husk-based activated carbons by urea at the 2:1 and 3:1 carbon/urea mass ratio.

Textural parameters calculated from the nitrogen isotherms of urea-modified samples are presented in Table 4.

Table 4. Textural parameters of urea-modified carbon samples calculated from the nitrogen isotherms.

Sample	S_{BET} (m^2/g)	C_{BET}	Total Pore Volume (cm^3/g)	Micropore Volume (cm^3/g)	Mesopore Volume (cm^3/g)
Rice Husk act	738	497	0.449	0.266	0.183
Rice Husk/urea 2:1 (33%)	486	429	0.295	0.177	0.117
Rice Husk/urea 3:1 (25%)	622	494	0.354	0.228	0.125

As can be seen from Table 4, after urea-modification, the value of the specific surface area of activated carbon samples decreases, as well as the volume of micropores and mesopores. Moreover, the more urea is used in the modification, the lower the values of the mentioned above parameters. Thus, in the case of the Rice Husk/urea 2:1 modification variant, the specific surface area is reduced by 35%, and the total pore volume by 34%. These results indicate that urea-derived species are preferentially grafted onto the pore walls of the carbon material, initially affecting the mesopores and, at higher loadings, progressively reducing the accessible volume of both meso- and micropores to a similar extent.

In order to confirm the chemical modification of the oxygen groups by urea, we performed an FTIR analysis of the samples, the results of which are shown in Figure 13.

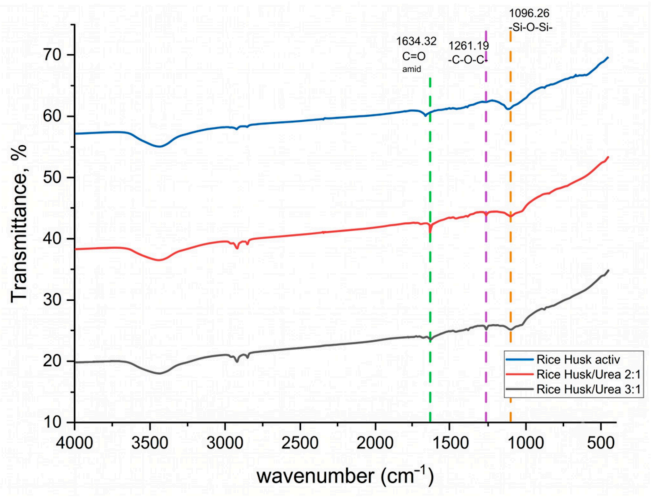


Figure 13. FTIR—spectra of the urea-modified activated carbon samples from Rice Husk.

Comparison of FTIR spectra of activated Rice Husk and urea-modified samples Rice Husk Urea 2:1 and Rice Husk Urea 3:1 revealed characteristic changes. In both urea samples, a negligible enhancement of the bands in the region of 3400 cm^{-1} is observed, which is associated with the introduction of amino groups (N–H) from urea. A pronounced peak in the region of 1634 cm^{-1} indicates the formation of carbonyl and/or amide structures, especially at a ratio of 3:1, where C–N vibrations are also enhanced (~1450 cm^{-1}). This confirms a positive nitrogen modification of the carbon surface. The presence of Si–O–Si bands (~1000–1100 cm^{-1}) is preserved in all samples, but their intensity is lower than that of activated Rice Husk, indicating possible partial leaching or chemical interaction with urea thermolysis products.

EDAX analysis results of urea-modified activated carbon from Rice Husk also confirm of presence of nitrogen-containing compounds (Figure 14).

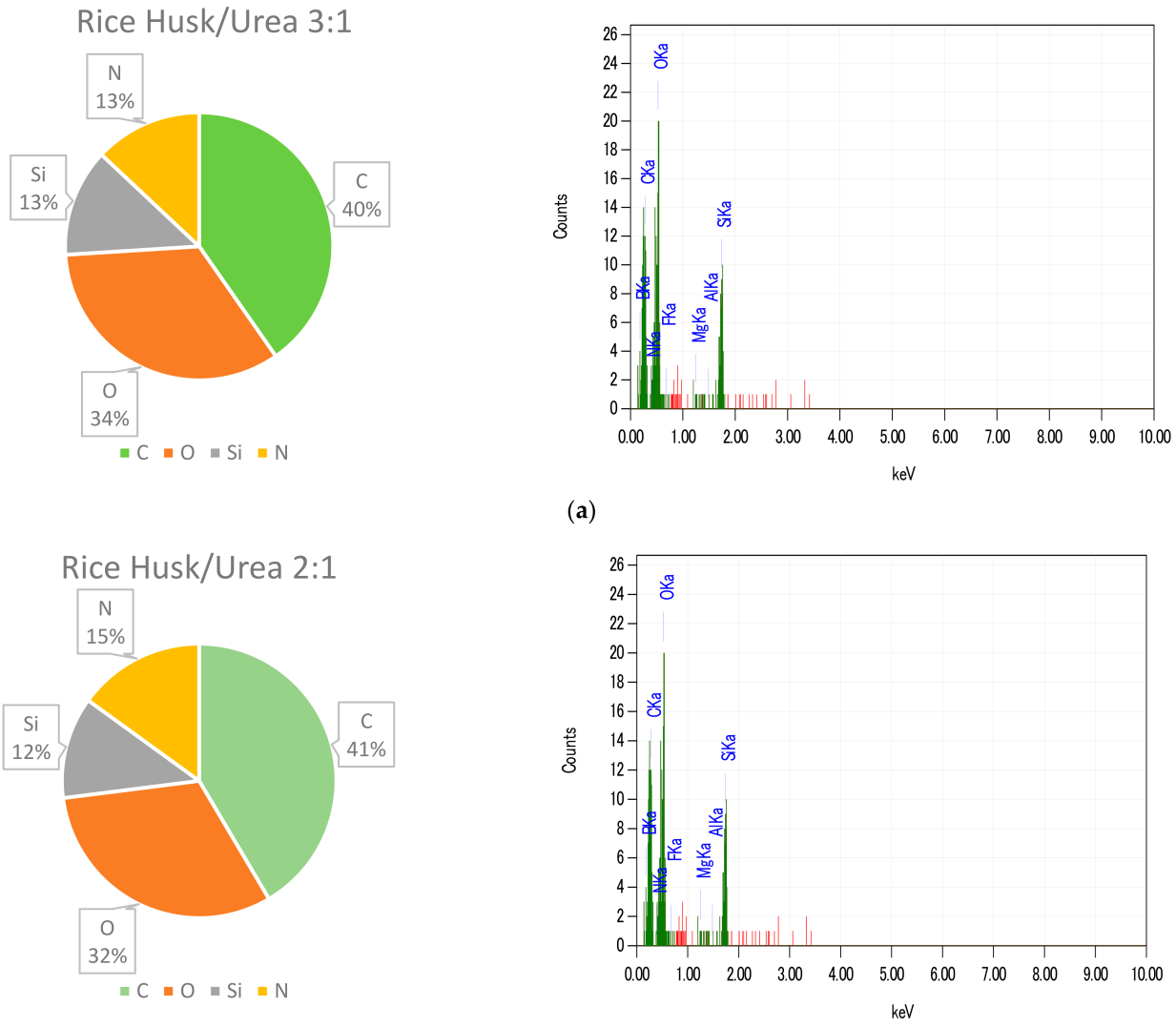


Figure 14. EDAX analysis results of the Rice Husk activated carbon samples modified by urea at ratio: (**a**) 3:1; (**b**) 2:1.

EDAX analysis of urea-modified carbon samples shows that increasing urea ratio from 25 (for 3:1 Figure 14a) to 33% (for 2:1 Figure 14b) by mass causes slight increasing (only 2% difference) of nitrogen atoms content in samples. The filling of pores with urea molecules is also confirmed by the analysis of urea adsorption isotherms on activated carbon—the SBET of activated carbon decreases from 738 to 486 m^2/g in the sample with 2:1 carbon/urea mass ratio (Table 3). Thus, from EDAX, SBET results and FTIR spectra, the chemical modification of the surface chemistry during the urea-modification process is confirmed.

3.4. Analysis of Sorption of SO_2

In order to study the effect of urea modification on the sorption of negatively charged toxic gases, we studied the sorption of SO_2 on activated and modified samples. The breakthrough curves are shown in Figure 15 and the breakthrough times presented in Table 5.

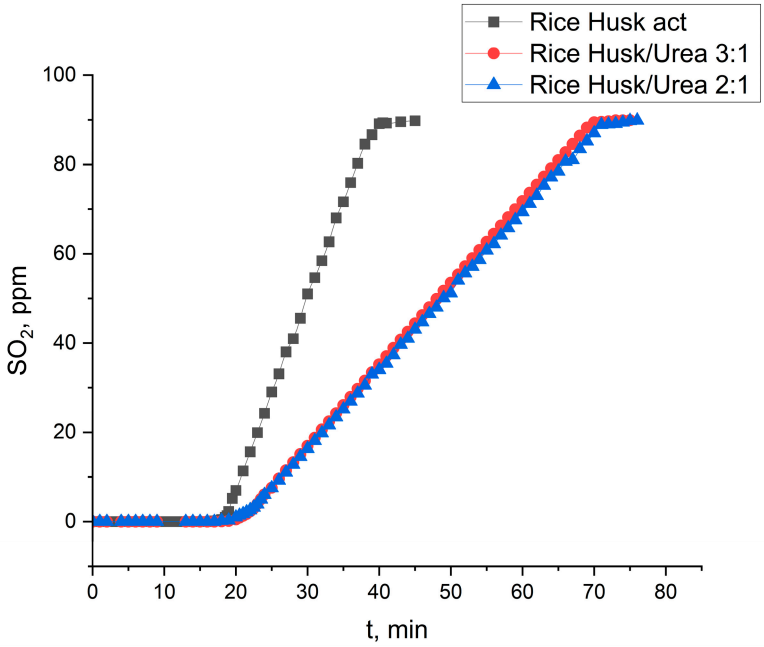


Figure 15. SO_2 breakthrough time curves of urea-modified carbon samples.

Table 5. SO_2 breakthrough times of activated carbon samples.

Samples	Breakthrough Time, min (SO_2—2 ppm)	Time (conc. SO_2—6 ppm)
Rice Husk activ	17 min 45 s	20 min 40 s
Rice Husk/urea 2:1	21 min 30 s	25 min 10 s
Rice Husk/urea 3:1	22 min 32 s	25 min 14 s

The breakthrough time curves for urea-modified Rice Husk samples showed that the modification increases the SO_2 breakthrough time by an average of 4 min. This indicates that, in addition to the physiosorption of gas molecules on the sorbent, chemical modification with urea provides an additional contribution to increasing the breakthrough time. This effect is particularly relevant for SO_2, whose adsorption is known to involve not only physiosorption but also chemisorption processes, especially through interactions with surface functional groups and nitrogen species introduced by modification [34]. At the same time, an increase in the urea content during sorbent modification does not lead to significant changes in this indicator. Apparently, the ratio of sorbent and urea 3:1 is sufficient to modify the surface of the sorbent and at the same time the pores of the sorbent are not clogged with urea-derived molecules and are suitable for sorption of other substances and gases. According to the classification in [35], gas masks based on urea-modified carbon from Rice Husks can be classified as class and type E2.

The experimental breakthrough curves of SO_2 adsorption were further analyzed using the Thomas and Yoon–Nelson models. The calculated kinetic parameters are summarized in Table 6.

The results demonstrate that surface modification with urea leads to a significant increase in the total dynamic sorption capacity towards SO_2 compared to the non-modified sample under the applied testing conditions (inlet concentration of 90 ppm, volumetric flow rate of 7.8 L/min, sorbent bed mass of 3.0 g, and relative humidity of 50%). For the initial Rice Husk activ, the experimental capacity was found to be 17.73 mg/g (0.277 mmol/g). Upon modification at a 3:1 mass ratio, the sorption capacity rose to 27.81 mg/g (0.434 mmol/g). A further increase in the modifier content to a 2:1 ratio resulted in a marginal change in performance, yielding a capacity of 28.42 mg/g (0.444 mmol/g).

This stabilization of capacity indicates that a 3:1 ratio is sufficient for optimal surface functionalization, whereas a higher urea concentration (2:1) does not provide additional active sites. Both the Thomas and Yoon–Nelson models exhibit good correlation, indicating their adequacy in describing the SO_2 dynamic filtration process under these fixed experimental parameters. A close agreement is observed between the calculated theoretical capacities from the Thomas model and the experimental values obtained via curve integration, confirming the validity of the applied mathematical approach.

Table 6. Kinetic parameters of SO_2 dynamic adsorption on initial and urea-modified Rice Husk sorbents modeled by Thomas and Yoon–Nelson equations.

Sample	q_{total} Experimental (mg/g)	τ, Experimental, (min)	Thomas Model		Yoon–Nelson Model	
			k_{Th} (L/mg × min)	q_{total} (mg/g)	k_{YN}, (L/min)	τ_{YN}, (min)
Rice Husk activ	17.73	29.0	0.098	17.62	0.023	29.0
Rice Husk/Urea 2:1	27.81	45.5	0.052	27.71	0.012	45.4
Rice Husk/Urea 3:1	28.42	46.0	0.048	28.33	0.011	46.5

To provide a deeper insight into the chemical mechanism governing the enhanced SO_2 retention on urea-modified sorbents, high-resolution XPS analysis of the N 1 s region was carried out before and after the gas sorption experiments. The N 1 s spectrum of the initial modified sample (Figure 16a) exhibits three major contributions: pyridinic nitrogen at 399.53 eV, pyrrolic nitrogen at 400.08 eV, and a minor component of tertiary/quaternary nitrogen at 401.55 eV.

Following exposure to the SO_2 gas stream, the chemical state of the surface nitrogen underwent substantial transformations (Figure 16b). The most remarkable feature is the increase in the peak area located at 402.42 eV, assigned to the tertiary/protonated nitrogen species. In carbonaceous sorbents, such a significant shift toward higher binding energies is a clear fingerprint of the formation of acid-base complexes where basic pyridinic sites donate electron density to accept acidic SO_2 molecules. This chemisorption mechanism is further corroborated by the emergence of a well-defined oxidized nitrogen peak at 403.97 eV [35].

Figure 16c illustrates the high-resolution XPS S 2p spectrum of the modified carbon material after SO_2 sorption. To accurately identify the chemical states of the captured sulfur species, the spectrum was deconvoluted into distinct spin–orbit doublets (S $2p_{3/2}$ and S $2p_{1/2}$) with a standard splitting energy of 1.2 eV and a constrained 2:1 peak area ratio. Additionally, a well-resolved high-energy doublet at 170.2 eV (S $2p_{3/2}$) and 171.4 eV (S $2p_{1/2}$) corresponds to sulfate species. The formation of a minor amount of sulfate species at room temperature is attributed to the presence of nitrogen functional groups. It is well-documented that N-doping introduces highly active defect sites that facilitate the activation of ambient or co-adsorbed oxygen, driving the partial surface oxidation of chemisorbed sulfite even under ambient conditions [36]. The absence of low-energy peaks in the 163–165 eV range confirms that the retained sulfur is completely stabilized in its oxidized forms, providing direct, non-speculative proof of the chemisorption pathway.

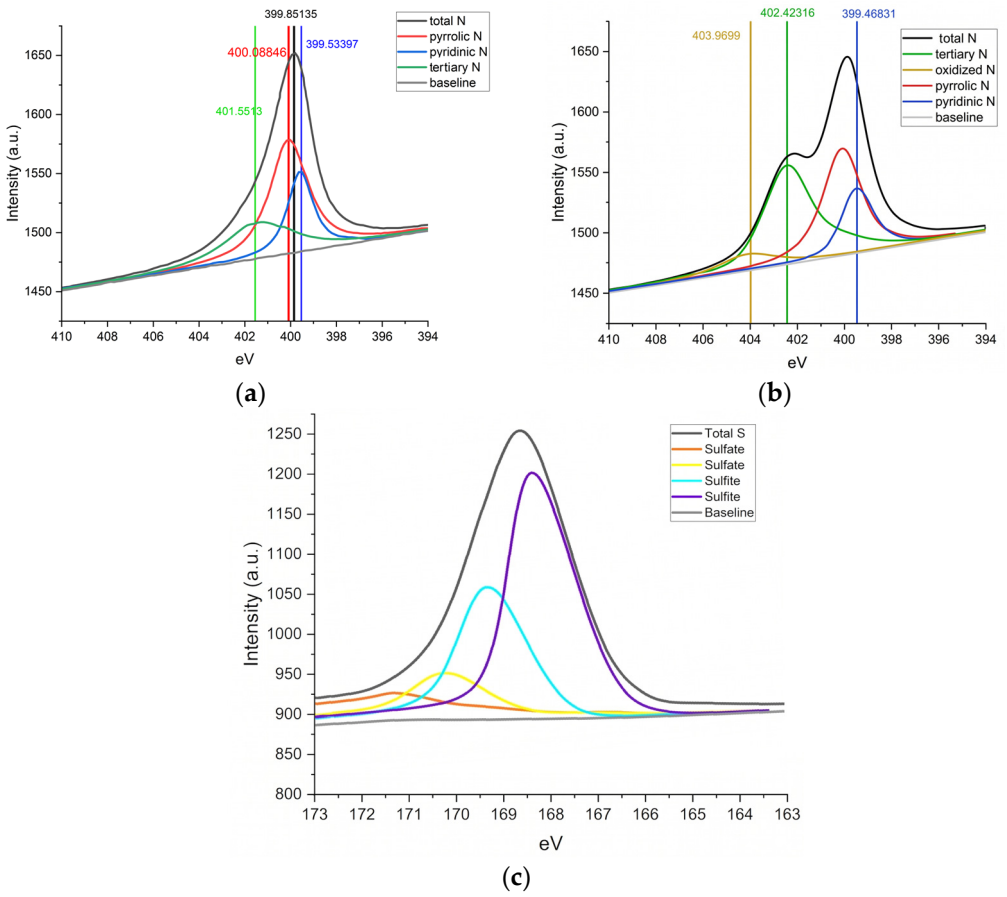


Figure 16. High-resolution XPS spectra of the urea-modified Rice Husk activated carbon sample: (**a**) N 1 s before SO_2, (**b**) after SO_2 sorption (**c**) S 2p after SO_2 sorption.

3.5. Cyclic Stability and Regeneration Performance

To evaluate the practical potential of the urea-modified Rice Husk sorbents, their performance over five consecutive adsorption-regeneration cycles was investigated (Table 7).

Table 7. Cyclic performance of the urea-modified Rice Husk/Urea 3:1 sorbent over five consecutive adsorption-regeneration cycles.

Cycle	SO_2 Adsorption Capacity, mg/g	Retention Rate, %
1	28.45	100.0
2	27.65	97.3
3	26.98	94.9
4	25,84	90.9
5	24.89	87.6

The results shown in Table 7 demonstrate the high stability of the material under operating conditions. Despite a slight decrease in the adsorption capacity (from 28.45 to 24.89 mg/g), the Rice Husk/Urea 3:1 sample retained about 87.6% of its initial effectiveness after the fifth cycle. The observed gradual decrease in capacity is due to partial thermal degradation of the most labile nitrogen-containing functional groups at a regeneration temperature of 400 °C. However, the fact that the vast majority of active centers remain active confirms the chemical stability of the N-doped carbon frame.

Thus, experiments show that the activated and urea-modified sorbents could be effective materials for gas mask production. The experimental results served as the basis for submitting an application and obtaining a patent for the invention of the Republic of Kazakhstan "Method for producing carbon sorbent" [37].

4. Conclusions

Among the different waste biomass precursors investigated, this study demonstrated that Rice Husk-based activated carbon exhibited the highest total pore volume and a well-developed interconnected porous structure (composed of macro-, meso- and micropores), together with a suitable composition and surface chemistry. These features resulted in superior sorption performance toward polar and positively charged gases, particularly ammonia, enabling classification of Rice Husk-based sorbents as K2-type materials according to EN standards. Chemical modification of Rice Husk activated carbon with urea further enhanced SO_2 breakthrough times, confirming that surface functionalization contributes significantly to chemisorption in addition to physical adsorption. Importantly, increasing the urea content beyond a 3:1 sorbent-to-urea ratio did not yield substantial additional benefits, indicating an optimal modification level that preserves pore accessibility. For the two gases studied, the hydrophobicity of this material contributed to improved performance under humid conditions, which are more representative of real operating environments. In particular, it reduces the competitive adsorption of water molecules, allowing the target gases to more effectively access and occupy the available sorption sites.

Additionally, Wheat Straw proved to be an effective precursor for the preparation of nanoporous carbons, whose highly developed microporous structure makes them particularly suitable for the removal of organic vapors such as cyclohexane. Overall, the results confirm that agricultural waste-derived activated carbons are promising, sustainable materials for gas purification and air filtration applications. The ability to tailor adsorption selectivity through precursor choice and surface modification highlights their strong potential for use in respirators, gas masks, and industrial emission control systems. Furthermore, the conversion of agricultural residues into activated carbons contributes to the recycling and valorization of biowaste streams, offering a cost-effective and environmentally sustainable approach to sorbent production. Future work should focus on long-term stability, regeneration efficiency, and performance under real operating conditions to support large-scale practical implementation.

5. Patents

Some of the results from the analysis of carbon samples from Rice Husks and walnuts formed the basis for the application and subsequent patenting of the invention “Method for Producing Carbon Sorbent” in the Republic of Kazakhstan. The patent number is 38053 and was granted on 29 May 2026.

Author Contributions: Conceptualization A.K. (Almagul Kerimkulova) and A.S.; methodology Y.Y., L.F.V. and A.Z.; validation G.N., V.Y., O.D.; formal analysis Z.M., V.Y. and M.A.; investigation Y.Y., N.A., A.Z., A.K. (Aisamal Kubaiden) and A.K. (Almagul Kerimkulova); writing—original draft preparation A.S. and A.K. (Almagul Kerimkulova); writing—review and editing A.S., L.F.V. and A.K. (Almagul Kerimkulova) visualization L.F.V. and M.A.; supervision A.S. and L.F.V.; project administration A.K. (Almagul Kerimkulova). All authors have read and agreed to the published version of the manuscript.

Funding: This work was supported by the Ministry of Science and Higher Education of the Republic of Kazakhstan grant (AP22786556).

Institutional Review Board Statement: Not applicable.

Informed Consent Statement: Not applicable.

Data Availability Statement: The original contributions presented in this study are included in the article. Further inquiries can be directed to the corresponding author.

Conflicts of Interest: The authors declare no conflicts of interest.

Abbreviations

The following abbreviations are used in this manuscript:

EDAX	Energy-dispersive X-ray spectroscopy
FTIR	Fourier Transform Infrared Spectroscopy
MFC	Mass Flow Rate Controller
VOCs	Volatile Organic Compounds
QSDFT	Quenched solid density functional theory

References

1. Mather, T.A. Volcanoes and the environment: Lessons for understanding Earth's past and future from studies of present-day volcanic emissions. *J. Volcanol. Geotherm. Res.* **2015**, *304*, 160–179. [CrossRef]
2. Yue, X.-L.; Gao, Q.-X. Contributions of natural systems and human activity to greenhouse gas emissions. *Adv. Clim. Change Res.* **2018**, *9*, 243–252. [CrossRef]
3. Perera, F. Pollution from fossil-fuel combustion is the leading environmental threat to global pediatric health and equity: Solutions exist. *Int. J. Environ. Res. Public Health* **2017**, *15*, 16. [CrossRef] [PubMed]
4. Gaffney, J.S.; Marley, N.A. The impacts of combustion emissions on air quality and climate—From coal to biofuels and beyond. *Atmos. Environ.* **2009**, *43*, 23–36. [CrossRef]
5. Hänninen, O.; Lehtomäki, H.; Korhonen, A.; Kokkola, T.; Hartikainen, A.; Sippula, O.; Haverinen-Shaughnessy, U.; Leviäkangas, P.; Rumrich, I.K. Health risks related to air pollution by transport categories and vehicle types: Comparison by mortality indicators. *Environ. Int.* **2025**, *202*, 109657. [CrossRef] [PubMed]
6. Badyelgajy, Y.; Doszhanov, Y.; Kapsalyamov, B.; Onerkhan, G.; Sabitov, A.; Zhumazhanov, A.; Doszhanov, O. Calculation of greenhouse gas emissions from tourist vehicles using mathematical methods: A case study in Altai Tavan Bogd National Park. *Sustainability* **2025**, *17*, 6702. [CrossRef]
7. Lizarazo Salcedo, C.G.; Whitehead, L.; Perkins, J.L.; Upegui-Rincón, S.; Guarguati-Ariza, J.; Quinchía, R.; Espinosa-Guerra, C.J. Management of acute exposure to toxic gases in the oil & gas industry—A practical approach. *Arch. Environ. Occup. Health* **2021**, *76*, 385–392. [CrossRef] [PubMed]
8. Tan, T.; Xu, X.; Gu, H.; Cao, L.; Liu, T.; Zhang, Y.; Wang, J.; Chen, M.; Li, H.; Ge, X. The characteristics, sources, and health risks of volatile organic compounds in an industrial area of Nanjing. *Toxics* **2024**, *12*, 868. [CrossRef] [PubMed]
9. Manono, B.O. Methane emissions from livestock operations: Sources, sinks, and mitigation strategies. *Methane* **2026**, *5*, 7. [CrossRef]
10. Sabitov, A.; Ibragimova, N.; Lyu, M.; Bolatova, D. About the need for developing risk management for ensuring safety from antibiotic and veterinary drug residues in Kazakhstan. *J. Sustain. Sci. Manag.* **2021**, *16*, 303–315. [CrossRef]
11. Amin, M.S.R. A critical review of pharmaceutical pollutants in soil and air: Ecotoxicological impacts on animal, plant and microbial communities—Health hazards and waste management. *Environ. Pollut. Manag.* **2026**, *3*, 70–87. [CrossRef]
12. Stegenta-Dąbrowska, S.; Galik, M.; Bednik-Dudek, M.; Syguła, E.; Kosiorowska, K.E. Applying compost biochar for gas adsorption—Effects of pyrolysis conditions. *Molecules* **2025**, *30*, 3365. [CrossRef] [PubMed]
13. Zhumanov, M.A.; Baizhumanov, K.D.; Doszhanov, O.M. Mobile Device for Cleaning Harmful Emissions in Atmospheric Air. Patent for Invention of Republic of Kazakhstan №34869, 12 February 2021.
14. Ringsby, A.J.; Ross, C.M.; Maher, K. Sorption of soil carbon dioxide by biochar and engineered porous carbons. *Environ. Sci. Technol.* **2024**, *58*, 8313–8325. [CrossRef] [PubMed]
15. Shi, J.; He, J.; Sheng, L.; Wu, X.; Mao, S.; Zhang, Y.; Xiang, C.; Sun, L. Stimuli-Responsive Multicolor Nacre-Mimetic Phosphorescent Bionanocomposite Thin Films via Network-Confinement Coupling. *Adv. Mater.* **2026**, *38*, e17075. [CrossRef] [PubMed]
16. Shi, J. pH-responsive collagen nanocomposite films reinforced by curcumin-loaded Laponite nanoplatelets for dynamic visualization of shrimp freshness. *Food Hydrocoll.* **2024**, *157*, 110447.
17. Jandosov, J.; Chenchik, D.; Baimenov, A.; Silvestre-Albero, J.; Bernardo, M.; Azat, S.; Doszhanov, Y.; Sabitov, A.; Busquets, R.; Howell, C.; et al. Assessment of phenolic and indolic compounds removal from aqueous media using lignocellulose-derived surface-modified nanoporous carbon adsorbents: A comparative study. *Int. J. Mol. Sci.* **2026**, *27*, 804. [CrossRef] [PubMed]
18. Zhan, M.-X.; Liu, Y.-W.; Ye, W.-W.; Chen, T.; Jiao, W.-T. Modification of activated carbon using urea to enhance the adsorption of dioxins. *Environ. Res.* **2022**, *204*, 112035. [CrossRef] [PubMed]
19. *ISO 10121-1:2014*; Test Method for Assessing the Performance of Gas-Phase Air Cleaning Media and Devices for General Ventilation—Part 1: Gas-Phase Air Cleaning Media. International Organization for Standardization: Geneva, Switzerland, 2014. Available online: https://www.iso.org/standard/51372.html (accessed on 3 November 2025).

20. Zeng, G.; Guo, S.; Zhai, X. Experimental study on adsorption of SO_2 and NH_3 by activated carbon with monometallic active sites at low concentration under room temperature. *ACS Omega* **2024**, *9*, 5523–5533. [CrossRef] [PubMed]
21. Jandosov, J.M.; Mansurov, Z.A.; Bijsenbayev, M.A.; Tulepov, M.I.; Ismagilov, Z.R.; Shikina, N.V.; Ismagilov, I.Z.; Andrievskaya, I. Synthesis of microporous-mesoporous carbons from rice husk via H_3PO_4-activation. *Adv. Mater. Res.* **2013**, *602*, 85–89. [CrossRef]
22. Teo, C.Y.; Jong, J.S.J.; Chan, Y.Q.; Oueslati, W. Carbon-based materials as effective adsorbents for the removal of pharmaceutical compounds from aqueous solution. *Adsorpt. Sci. Technol.* **2022**, *2022*, 3079663. [CrossRef]
23. Ioni, Y.; Ibragimova, V. Study of sorption activity of carbon nanomaterials for capture of chlorine-containing gases. *Clean Technol.* **2025**, *7*, 39. [CrossRef]
24. Akhmetzhanova, D.; Sabitov, A.; Doszhanov, Y.; Atamanov, M.; Saurykova, K.; Zhumazhanov, A.; Atamanova, T.; Kerimkulova, A.; Velasco, L.F.; Zhumagalieva, A.; et al. Zeolites and activated carbons in hydroponics: A systematic review of mechanisms, performance metrics, techno-economic analysis and life-cycle assessment. *Sustainability* **2025**, *17*, 10977. [CrossRef]
25. Pamula, K.; Pophali, A.; Gersappe, D.; Kim, T. In-situ Raman spectroscopic analysis of phase transition temperatures in silica interacting with water and NaCl solutions. *Sci. Rep.* **2025**, *15*, 26449. [CrossRef] [PubMed]
26. Kuloglija, S.; Gohary Ahmed, A.E.; Jordan, C.; Golda, M.; Ipsmiller, W.; Steinacher, N.; Winter, F.; Meitner, D.; Luckeneder, A.; Harasek, M. Sustainable Activated Carbon Production from Sunflower Seeds via Chemical Activation. *Sustainability* **2025**, *17*, 2568. [CrossRef]
27. Liu, L.; Tan, S.J.; Horikawa, T.; Do, D.D.; Nicholson, D.; Liu, J. Water adsorption on carbon—A review. *Adv. Colloid Interface Sci.* **2017**, *250*, 64–78. [CrossRef] [PubMed]
28. Verbruggen, N.; Hermans, C. Physiological and molecular responses to magnesium nutritional imbalance in plants. *Plant Soil* **2013**, *368*, 87–99. [CrossRef]
29. Cakmak, I.; Kirkby, E.A. Role of magnesium in carbon partitioning and alleviating photooxidative damage. *Physiol. Plant.* **2008**, *133*, 692–704. [CrossRef] [PubMed]
30. Ćwieląg-Piasecka, I.; Jamroz, E.; Medyńska-Juraszek, A.; Bednik, M.; Kosyk, B.; Pollákova, N. Deashed wheat-straw biochar as a potential superabsorbent for pesticides. *Materials* **2023**, *16*, 2185. [CrossRef] [PubMed]
31. Bakdash, R.S.; Aljundi, I.H.; Basheer, C.; Abdulazeez, I. Rice husk derived aminated silica for the efficient adsorption of different gases. *Sci. Rep.* **2020**, *10*, 19526. [CrossRef] [PubMed]
32. Bazan-Wozniak, A.; Nowicki, P.; Wolski, R.; Pietrzak, R. Activated bio-carbons prepared from the residue of supercritical extraction of raw plants and their application for removal of nitrogen dioxide and hydrogen sulfide from the gas phase. *Materials* **2021**, *14*, 3192. [CrossRef] [PubMed]
33. Ramirez-de-Arellano, J.M.; Canales, M.; Magaña, L.F. Carbon nanostructures doped with transition metals for pollutant gas adsorption systems. *Molecules* **2021**, *26*, 5346. [CrossRef] [PubMed]
34. Bagreev, A.; Bashkova, S.; Bandosz, T.J. Adsorption of SO_2 on Activated Carbons: The Effect of Nitrogen Functionality and Pore Sizes. *Langmuir* **2002**, *18*, 1257–1264. [CrossRef]
35. *EN 14387:2004+A1:2008*; Respiratory Protective Devices—Gas Filters and Combined Filters—Requirements, Testing, Marking. European Committee for Standardization: Brussels, Belgium, 2008.
36. Zhang, C.; Lin, W.; Zhao, Z.; Zhuang, P.; Zhan, L.; Zhou, Y.; Cai, W. CVD synthesis of nitrogen-doped graphene using urea. *Sci. China Phys. Mech. Astron.* **2015**, *58*, 107801. [CrossRef]
37. Kerimkulova, A.R.; Mansurov, Z.A.; Ermoldanov, E.Z.; Asanbek, N.M.; Aidarbek, A.E.; Sabitov, A.N. Method for Producing Carbon Sorbent. Patent for Invention of Republic of Kazakhstan №38053, 29 May 2026.

Disclaimer/Publisher's Note: The statements, opinions and data contained in all publications are solely those of the individual author(s) and contributor(s) and not of MDPI and/or the editor(s). MDPI and/or the editor(s) disclaim responsibility for any injury to people or property resulting from any ideas, methods, instructions or products referred to in the content.